SAND2022-3437C

Differential Cancellation Based RF Switch Enabling High Isolation and Minimal Insertion Loss in 0.0006 mm^2 Area

Travis Forbes[1], Justine Saugen, Benjamin Magstadt
Sandia National Laboratories, USA
[1]tmforbe@sandia.gov

***Abstract*—An RF switch technique applying differential signal cancellation is presented. The proposed approach enables high isolation and extremely small size by employing cascode current steering within a differential amplifier. Unlike series RF switches, isolation is limited by device mismatch, not switch parasitic capacitance, enabling high frequency operation. Since the switch is within the already present cascode devices, there is no additional insertion loss from the switch. The switch was implemented in a 180 nm CMOS process within an amplifier as part of an on-chip receiver and achieves 36-43 dB isolation across 0.5-2 GHz, while occupying an area of only 0.0006 mm^2.**

***Index Terms*—RF switch, isolation, current steering, CMOS**

I. Introduction

Radar systems targeting long distance operation, such as those used for weather radar, must receive and process RF reflections with good signal-to-noise ratio (SNR) from objects >50 miles away. Such systems employ high transmit power and highly directional antennas to maintain good SNR but are sensitive to leakage between the transmit and receive paths through EM coupling inside the enclosed radar module and through power supplies. Such leakage can create a high gain positive feedback loop between the transmit and receive paths which can cause the circuits to oscillate, especially during high power transmit events. To prevent oscillation, RF switches are placed between amplifiers in both the transmit and receive paths where only one path is enabled at a time and the disabled path is desired to have no gain in order to prevent any positive loop gain from forming (Fig. 1). A similar approach is used in radar systems which employ off-chip high quality factor filters in the receiver which have a long impulse response time, where isolation switches prevent large pulse injection into these filters during transmit events to enable fast pulsing operation. While series RF switches have shown good performance when employed at the antenna interface to switch the connection between the antenna and the transmitter/receiver [1]–[4], a conventional radar design employs the same switches between amplifiers for isolation (Fig. 1a). However, these series RF switches have significant insertion loss which must be overcome by additional amplification and power consumption, have limited isolation, and are physically large in size.

To solve these challenges, this paper proposes to integrate the RF isolation switch operation into the amplifier designs (Fig. 1b). The proposed RF switching approach employs current steering in the differential amplifier cascode devices to cancel the RF signal at each of the differential outputs. The differential approach enables high isolation limited only by device matching which may be calibrated unlike conventional series switches which are limited by device parasitics. The approach also has no inherent high frequency isolation degradation, has DC operating point preserving operation for high switching speeds, and enables extremely small size integration within the amplifier cascode operation.

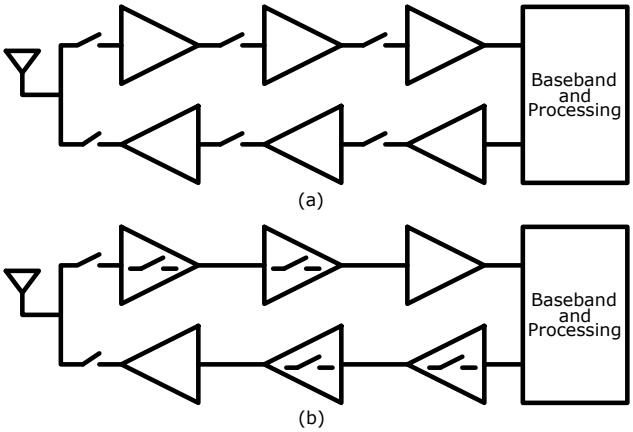

Fig. 1. RF amplifier configurations for high power radar systems: (a) conventional design with series RF switches between amplifiers and (b) proposed design with integrated switches within amplifier cascodes.

II. RF Switch Operation

Conventional series RF switches are constructed from a pass transistor (M_1) placed in the signal path and a shunt transistor (M_2) placed at the pass transistor output to ground (Fig. 2). In the enabled state, M_1 is enabled while M_2 is disabled, with insertion loss set by the resistance of M_1 compared to the impedance seen looking into the next RF circuit block. In the disabled state, M_1 is disabled and M_2 is enabled, where M_1 provides a high signal path impedance and M_2

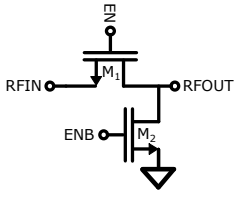

Fig. 2. Conventional series RF switch configuration.

978-1-6654-8609-5/22/$31.00 ©2022 IEEE

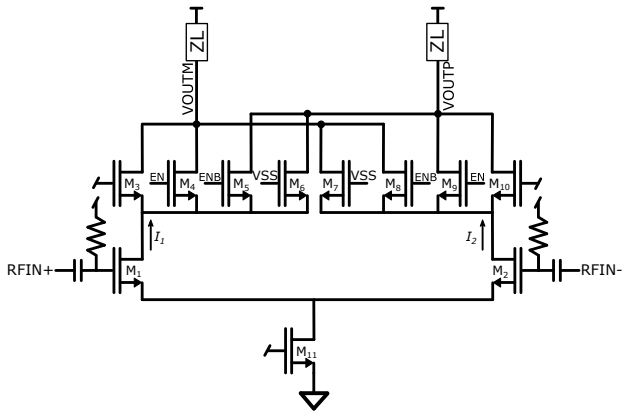

Fig. 3. Example differential amplifier employing the proposed differential cancellation based RF switch technique.

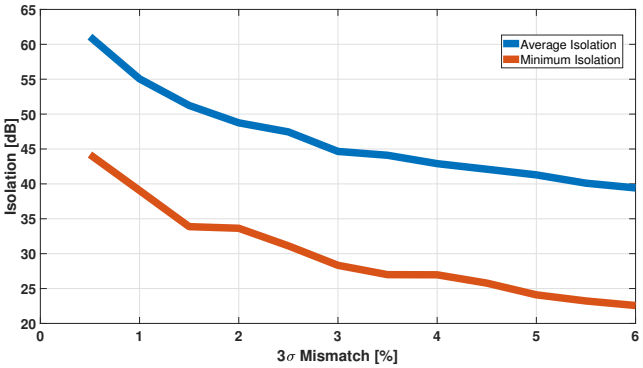

Fig. 4. Average and minimum isolation versus 3σ device mismatch for the differential cancellation based switch technique across 1000 monte carlo simulation points.

provides a small impedance at the output of M_1 to ground. While the disabled state resistance of M_1 is high, the drain-to-source capacitance C_{ds} of M_1 forms a high pass filter with the ON resistance of M_2, thus creating a high pass filter. This high pass filter results in reduced isolation with increased RF frequency as can be seen in the measured performance of prior work (e.g. [1], [2]).

An example differential amplifier employing the proposed approach is shown in Fig. 3, while other cascode amplifier configurations including balun and pseudo-differential may be implemented with the same principal described here. In the proposed approach, the cascode device of width W is split into four parallel devices, each of width W/2 (M_3-M_6). The input voltage is converted to an inverted current I_1 by the transistor M_1. Transistors M_3-M_4 connect the current I_1 to the output of the same polarity ($VOUTM$), while M_5 connects the current I_1 to the output of opposite polarity ($VOUTP$) in the first differential circuit half. The same configuration, with opposite polarities, is used in the other differential circuit half. In the enabled state, the amplifier operates as a conventional cascode amplifier with all input current steered to the output of same signal polarity by applying the cascode bias voltage to EN and 0V (VSS) to ENB. As a result, there is no insertion loss in the enabled state as long as the output load is tuned for the added total drain capacitance of the disabled cascode devices. In the disabled state, half the current of each input polarity is steered to each differential output, ideally providing no amplifier gain from the input to each of the differential outputs. In both cases, a disabled device M_6 is included for symmetry in the cancellation operation. Note in the disabled and enabled states, power consumption in the amplifier is the identical thus no added power consumption is consumed by this approach in the same way as the series RF switch approach.

Unlike the series RF switch configuration, here the only high frequency leakage path is through the C_{ds} of the disabled cascode devices. By including the always disabled device M_6 (and M_7), the capacitive leakage is symmetric between both differential cancellation paths, making cancellation constant across frequency. A simulation with real devices including no mismatch confirmed this frequency independent cancellation, showing infinite isolation across 0.2-60 GHz. The isolation achieved is ultimately limited by mismatch in the differential amplifier and cascode devices. Fig. 4 shows the average and worst case (3σ) isolation performance of the approach across device mismatch. Since the isolation can be made flat across frequency and is limited by device mismatch, isolation may be further enhanced by calibrating the differential mismatch through additional, smaller, cascode devices placed in parallel to the cancellation cascode devices to adjust the cancellation current strengths to each differential output from each differential input. Such an approach would still rely on differential symmetry in following circuits to cancel gain imbalance from the differential common source devices at each differential output. For complete isolation calibration, both the cascode calibration described, as well as calibration of the transconductance of the differential common source devices would enable ideal cancellation at each differential output. Such calibration could be completed by adjusting the device bias points or by having parallel devices to the main devices which could be enabled/disabled by a switch at their source node. Calibration to improve isolation is not possible using a series switch approach as the isolation is limited by device parasitics.

Another challenge with placing the series RF switch between two amplifiers is perturbation of the DC operating point. In the conventional approach, a DC blocking capacitor is required prior to the series RF switch to keep the DC level at the switch node at 0V since in the disabled state the shorted transistor M_2 will force DC voltage to 0V. If the DC blocking capacitor is not included, the output node of the series switch which connects to the DC blocking capacitor at the next amplifier input would be required to charge back to the previous amplifier's output voltage when transitioning to the enabled state prior to normal circuit operation, limiting switching time. The proposed differential cancellation based RF switch approach has no change in DC bias voltage at the source or drain nodes of the cascode switch, therefore saving

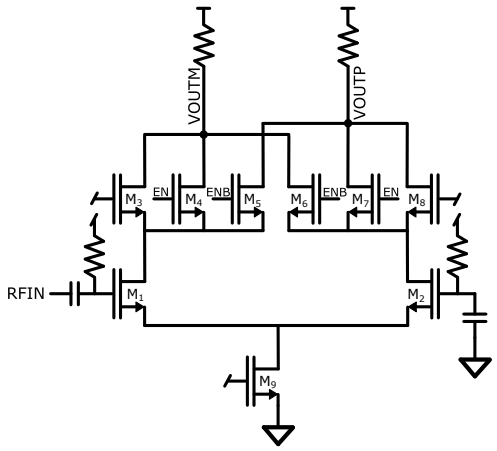

Fig. 5. Example implementation of the proposed approach within an intermediate frequency balun amplifier.

significant area by removing the DC blocking capacitor at the input side of the switch and enabling fast switch transition time. Since the approach can be completed in CMOS, the switch can be directly implemented on-chip with other receiver and transmitter circuits, can be controlled with standard CMOS control voltages, and can be implemented with extremely small area overhead.

III. Example Circuit Implementation

The proposed approach was implemented, in part, within the high intermediate frequency (IF) portion of an RF receiver. The cascode switching technique was employed in a single-to-differential balun amplifier targeting operation from 0.5-1 GHz as shown in Fig. 5. The intended application required modest isolation in each amplifier and was able to be achieved with no calibration. However, common centroid layout techniques were used in the design to achieve good matching performance. Since the implemented block was targeting frequencies below 1 GHz, the additional cascode devices ($M_6 - M_7$ in Fig. 3) were not included for area savings as simulation showed capacitive symmetry effects on isolation would not reduce performance until approximately 1.5 GHz. Both calibration and the addition of $M_6 - M_7$ in Fig. 3 may be included as described in Section II for further increased bandwidth and switch isolation performance.

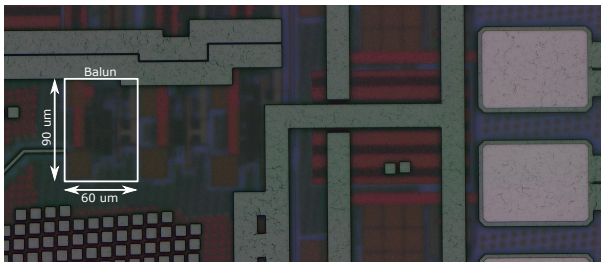

Fig. 6. Die micrograph of the implemented balun with differential cancellation switch.

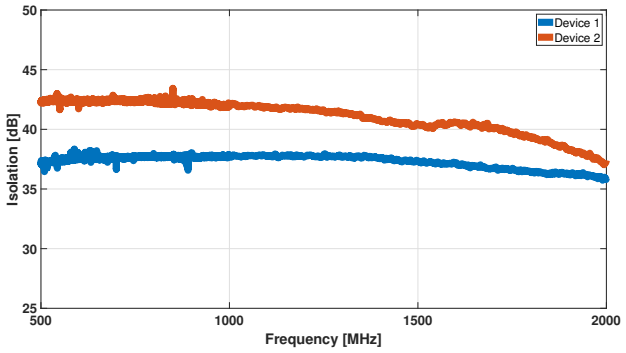

Fig. 7. Measured isolation performance of 2 sample devices across 0.5-2 GHz.

TABLE I
Performance Summary and Comparison to Prior Art.

	This Work	RFIC 2020 [1]	MTT 2013 [2]
Architecture	Differential Cancellation	Series Switch	Series Switch
Frequency	0.5-2 GHz	0.4-5.5 GHz	1-60 GHz
Isolation	36-43 dB[1]	40-70 dB	23-50 dB
Insertion Loss	None	0.3 dB	0.7-2.5 dB
Can Calibrate Isolation?	Y[1]	N	N
DC Preserving?	Y	N	N
Control Voltage	1.8V	-8V	1V
Technology	180 nm CMOS	GaN SLCFET	45 nm SOI CMOS
Active Area	0.0006 mm^2	3.38 mm^2	0.04 mm^2

[1]Technique enables calibration but was not implemented in measurement circuit.

IV. Measured Performance

The circuit in Fig. 5 was implemented in a 180 nm CMOS process in the IF section of an RF receiver. The die micrograph of the block design is shown in Fig. 6 and the active area of the amplifier was 0.0054 mm^2 and the cascode switching circuitry consumed only 0.0006 mm^2 area. Note the area overhead of the proposed approach is even smaller as much of the active area would already have been consumed by the cascode devices in the same amplifier without the proposed switch technique. The cascode switching technique adds no additional power consumption to the balun amplifier, similar to using a series switch technique, and the balun consumes 2.4 mW from a 1.8V supply.

Isolation performance of the example balun circuit was measured across 2 devices from 0.5-2 GHz and the results are shown in Fig. 7. Flat isolation of >36 dB was achieved from 0.5-2 GHz, while isolation begins to roll off around 1.5 GHz as was also found in simulation as mentioned in Section III. Employing additional cascode devices for capacitive symmetry (M6-M7 in Fig. 3) can be employed for higher frequency operation. While 2 devices are measured here, uncalibrated performance is expected to follow performance described in Fig. 4 given a larger sample size, while calibration may be included for increased performance as described in Section II.

The measurement results of the example circuit implementation are compared to other RF switching techniques in Table

I. The example device shows similar isolation as the conventional series switches with significantly lower active area. The proposed approach also enables no added insertion loss, DC preserving operation, requires only a CMOS compatible control voltage, and, while not implemented in the example circuit, can be calibrated for further increased isolation performance. While shown here at low GHz frequencies, the proposed technique may be employed at much higher RF frequencies using the techniques described in this paper to achieve high isolation at high frequency using calibration and capacitive device symmetry.

V. Conclusion

An RF switch technique based on differential signal cancellation was presented. The approach enables high isolation which has no inherent high frequency degradation and which may be calibrated for increased performance. The switch may be integrated within already present cascode amplifier designs for minimal area overhead and can provide fast switching operation by preserving DC bias voltages. An example circuit employing the approach showed 36-43 dB isolation from 0.5-2 GHz with no calibration.

Acknowledgment

The authors thank JJ Juarez and Tyler Wortman for board assembly, test code creation, and testing support.

References

[1] J. Hug, J. Parke, and V. Kapoor, "A 100 W UHF to S-band RF switch in the super-lattice castellated field effect transistor (SLCFET) 3S process," *2020 IEEE Radio Frequency Integrated Circuits Symposium (RFIC)*, 2020, pp. 71–74.

[2] M. Parlak and J. Buckwalter, "A passive I/Q millimeter-wave mixer and switch in 45-nm CMOS SOI," *IEEE Transactions on Microwave Theory and Techniques*, vol. 61, no. 3, pp. 1131–1139, 2013.

[3] C. Hill, C. Levy, H. AlShammary, A. Hamza, and J. Buckwalter, "RF watt-level low-insertion-loss high-bandwidth SOI CMOS switches," *IEEE Transactions on Microwave Theory and Techniques*, vol. 66, no. 12, pp. 5724–5736, 2018.

[4] U. Kodak and G. M. Rebeiz, "A 5G 28-GHz common-leg T/R front-end in 45-nm CMOS SOI with 3.7-dB NF and -30-dBc EVM with 64-QAM/500-MBaud modulation," *IEEE Transactions on Microwave Theory and Techniques*, vol. 67, no. 1, pp. 318–331, 2019.